NUMERICAL SIMULATIONS OF HYPOTHETICAL ENHANCED GEOTHERMAL SYSTEMS

Marco Cecioni and Michael O'Sullivan

Department of Engineering Science, University of Auckland, Private Bag 92019, Auckland, New Zealand

mcecioni@aurum.cl

m.osullivan@auckland.ac.nz

Keywords: *EGS, numerical modelling*

ABSTRACT

Numerical simulations of hypothetical enhanced geothermal systems (EGS) have been carried out in order to be able to understand what to expect from them in terms of power production. Since the quantity of unconventional geothermal resources in the world is larger than that of conventional resource it is a topic worthy of study. In this study simulations were carried out with different shapes for the cloud of fractures, with different numbers of production wells (1 to 4) and various injection rates (5 to 30 kg/s). The best set of parameters was found to be a configuration of 1 injection well in the centre of the cloud surrounded by 4 production wells located above the injector. This configuration produced a power output of 1.1 MWe.

1. INTRODUCTION

1.1 Background on EGS

The idea of an Enhanced or Engineered Geothermal System (EGS) dates back to the early work at Fenton Hill (Brown, 2009), but there has been renewed interest in it since the MIT study of its potential (Tester, 2006). There has also been some negative comment on EGS and the issues were well summarised by Pritchett (2012) who concluded positively: "There's *plenty* of hot rock down there."

The idea of an EGS is simple:

(i) Create a zone of artificial permeability in rock at high temperatures by drilling a deep well and pumping in cold water to fracture the rock
(ii) Drill a second well to intersect the fractured zone
(iii) Pump cold water down one well and produce hot water from the second well.

A good EGS requires a large cloud of uniform fractures to provide the ideal underground heat exchange system. To date this ideal has not been achieved and for various reasons none of the past EGS projects have been commercially successful.

The two best-documented EGS projects are Soultz-sous-Forets (e.g. Genter *et al*., 2009; Gentier *et al*., 2011) and the Cooper Basin (e.g. Chen & Wyborn, 2009; Yanagisawa *et al*., 2009; Hogarth and Bour, 2015; Holl and Barton, 2015). For both of them the post-stimulation (TH) behaviour has been modelled using TOUGH2 (Siffert *et al*., 2013; Llanos *et al*., 2015).

Recently there has been a considerable amount of research on modelling the thermo-hydro-mechanical (THM) problem of the development of the fracture cloud at Soultz-sous-Forets, Cooper Basin and elsewhere. This is probably the most important EGS modelling challenge but that is not the problem considered here. Instead only the post-stimulation, thermo-hydro, problem is considered.

This study aims to determine the power production potential of EGS projects for different shapes and sizes of a cloud of stimulated fractures in the reservoir in order to understand what to expect after permeability enhancement has been carried out. Different geometries of the cloud of stimulated permeability with different well configurations are modelled and the power output is determined in each case.

Two main model outputs are of most interest: the power output and the water loss in the system. Both are related to the shape of the enhanced permeability cloud, the injection rate and the number of production wells.

Some work has already been done on estimating the power production that can be achieved with EGS technology. For example, Chamorro *et al*. (2014) concluded that an output of 6560 GWe can be achieved in Europe by exploiting resources with temperatures above 150°C and at depths of up to 10 km. Also, Wu *et al*. (2013) stated that by 2050 the United States of America could be producing 100 GWe from EGS and other unconventional geothermal resources. At the Cooper Basin, Australia, Mills & Humphreys (2013) stated that, with 1000 square kilometres of hot granite resource, the EGS project could be scaled to produce several hundreds of megawatts. Currently the pilot project has been completed proving that electricity can be generated from an EGS resource in Australia, but on the other hand, the project has not proven to be profitable, so at the time of writing the power plant has been switched off, but is being maintained while waiting for further testing to occur.

Due to the nature of EGS projects, it is expected that comparatively low temperature water (say <200°C) will be produced and a binary power plant will be used to transform the mined heat into electricity. Recent projects such as Habanero in Australia (Mills & Humphreys, 2013), Desert Peak geothermal field in USA (Zeng *et al*. 2013), Soultz-Sous-Forêts, France (Held *et al*., 2014) have all used a binary power plant. The technologies to transform the heat into electricity will not be the focus on this paper and more information about different technologies can be found in the literature. The efficiencies of power plants given by Zarrouk & Moon (2014) is enough information for the scope of this report. These efficiencies do not consider reinjection pump power, and this is one of the main parasitic loads. Mills & Humphreys (2013) report that the 1 MWe plant of Habanero, Australia, uses ≈ 650 kWe to pump water underground at a rate of 17 kg/s, leaving the rest for external loads.

1.2 Fracture clouds

In this paper we use the term "a cloud of fractures" to describe the shape of the reservoir area that has been

stimulated. It is not within the scope of this paper to predict what kind of cloud of fractures is going to be created. Instead we consider some idealised special cases in order to understand how they behave and how we can monitor their behaviour.

Once the stimulation begins, the rock will fracture on the naturally weak planes (Kohl & Mégel, 2007; Zeng *et al.*, 2013). This means the orientation of the fracture cloud will be perpendicular to the minimum stress in the rock. An example of this is the Habanero EGS project in Australia. Habanero has a stress field at 4 km below the surface in which the vertical component is the smaller one. This is reflected by the stimulated volume forming a sub-horizontal cloud, as shown by the data published by McMahon & Baisch (2013).

The seismic monitoring system used by them gives enough information to allow the estimation of the size, orientation and even the propagation of the cloud during stimulation. The fracture clouds at Habanero extended progressively, showing that several stimulations can be used to create a large stimulated volume (Chen & Wyborn, 2009). However the economic benefit of the extra plant output that could be obtained by increasing the size of the fracture cloud must be balanced against the cost of the extra stimulations. Figure 1 shows the induced seismicity of Habanero project, where the different sizes of the spheres reflect the magnitude of the events. Chen & Wyborn (2009) say that the micro-seismic data reveals that the stimulated area is 4 km^2 and has a thickness between 10 and 100 meters, so the volume is in the range of 40 - 400 million cubic meters.

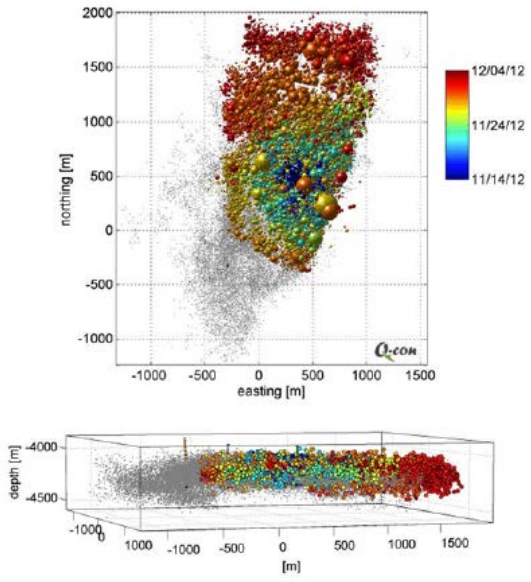

Figure 1: Cloud of fractures at Habanero EGS project (McMahon & Baisch, 2013).

Figure 2 shows a 3D model of the Soultz-Sous-Forêts project with the interpreted fractured area from micro-seismicity. In this case the total cloud volume (Sausse *et al.*, 2010) is estimated to be 5.55 km^3 (5,550 million cubic meters).

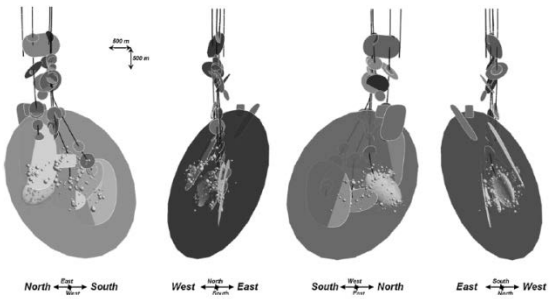

Figure 2: Interpretation of the fault system at Soultz-Sous-Forêts (Sausse et al., 2010).

The largest fracture cloud considered here has a volume 338 million cubic meters, comparable in size to the fracture cloud created at the Habanero project but smaller than that stimulated at Soultz-Sous-Forêts.

2. PREVIOUS MODELLING STUDIES OF EGS

Several models have been made for studying EGS projects, some of them simulating actual projects and others considering hypothetical cases. For the hypothetical models discussed in this report experiences from real projects were taken into account in order to try to make the results match reality.

A model produced by Bataillé, Genthon, Rabinowicz, & Fritz (2006) consists of a rectangular fractured reservoir (750 m long, 750 high and 35 m of wide), surrounded by impermeable granite, with adiabatic impermeable boundary conditions imposed on the sides. Rock properties are based on the Soultz-Sous-Forêts EGS project. These authors claim that if there is no free convection in an EGS reservoir then economic exploitation will end in a short time. However, it is expected that in an EGS reservoir the stimulated volume will not have enough permeability to allow free convection.

Butler et al. (2004) show conclusive results for an EGS development, results that were taken into account at the time of planning the research discussed in this report. These results show that higher permeability does not necessarily mean better production if the heat-transfer area is not enhanced. As well, for a given geometry, increasing the stimulated volume will result in higher output without a significant change in the generation profile and the average net generation for a certain volume is independent of well geometry. The models used by these authors consist of a rectangular block of fractured granite and reservoirs of different sizes and different well sets, using rock properties based on the Desert Peak EGS project, Nevada, USA. The model has peripheral aquifers in the top layers. A grid 3,657 m long 3,657 m wide and 1,524 m deep (12,000-12,000-5,000 feet) is used in order to reduce boundaries effects. The production method uses injection and production pumps. The authors also state that they simulate the production of more mass than is injected, obtaining a gain in fluid from the reservoir. In the present work only an injection pump is considered and part of the injected fluid is lost in the system.

Wu *et al.* (2013) and Zeng *et al.* (2013, 2014) conclude that the most significant parameters involved in power generation from an EGS project are water injection rate, reinjection temperature and reservoir permeability. For a single fracture, the heat transfer capacity of the rock is important (Zeng *et al.*, 2013) while in larger stimulated areas it is not such a relevant parameter (Wu *et al.*, 2013; Zeng *et al.*, 2014). The model used by Wu *et al.* (2013) consists of a

fractured granite rectangular reservoir (400 m high, 400 m wide and 500 m long) with impermeable layers above and below. Horizontal injection and production wells are used. The rock properties used are based on those for Desert Peak. Water losses are ignored.

A similar model has been set up for the Yangbajin geothermal field in China (Zeng *et al*., 2014). A cap and basement of impermeable rock are used and the reservoir is slightly fractured granite 1000 m long, 500 m wide and 400 m high, with the rock properties as found for granite at Yangbajin. All the boundary conditions are no-flow for mass and heat. The main point of difference in this model is that a single horizontal production well is used and that cold water is not injected since there is *in-situ* groundwater. A pump is used to extract the hot fluid from the horizontal well. Zeng *et al*. (2013) simulate a single fracture utilizing a suction pump in order to minimize fluid loss. The simulated granite reservoir used is a 400 m long, 500 m high and 0.002 m wide, simulating the fracture. The lateral boundary conditions are no-flow for mass and heat, and the temperatures and pressures of the uppermost and lowermost layers are fixed.

3. NUMERICAL MODEL

3.1 Discussion

The model considered here consists of a hypothetical HDR (hot dry rock) or EGS reservoir in which hydraulic stimulation has been used in order to obtain enough permeability to extract the heat. The rocks involved in this model are sediments and granite, which is a common setting for the HDR or EGS reservoirs as seen in actual projects. The modelled fracture cloud is located in the centre of the granite zone in the model and is assumed to have permeability ten times higher than the original. The enhanced permeability is considered to be constant during the lifetime of the project, and so seismic activity and mineral deposition are not taken into account (Bataillé *et al*., 2006; Wu *et al*., 2013).

The software used to run the simulation was AUTOUGH2_4. This is the University of Auckland's version of the software TOUGH2 (Pruess *et al.* 1999). The rock parameters for the model are shown in Table 1.

Table 1: Rock properties.

Rock	Sediment	Granite	Fractured granite
Density kg/m^3	2,500	2,500	2,500
Porosity	1%	1%	2%
Permeability m^2 (isotropic)	1.0E-15	1.0E-15	1.0E-14
Specific heat J/kg K	1,000	1,000	1,000
Thermal conductivity W/m K	2.2	2.7	2.7

3.2 Model design

The grid considered for this study is a rectangular grid, with finer resolution in the stimulated area. The grid size is similar to what has been used in other studies reported in the literature (Butler *et al*., 2004; Jiang *et al*., 2013; Kohl & Mégel, 2007; Llanos *et al*., 2015; Zeng *et al*., 2014). The actual size of the whole model is 3 km x 3 km x 3 km, with blocks of 40 m x 40 m x 40 m in the area of interest, *i.e.* in and around the fracture cloud. The sedimentary layer extends from the surface (0 m) to a thousand and ten meters below the surface (-1010 m), the rest of the model consists of granite (from -1010 m to -3000 m).

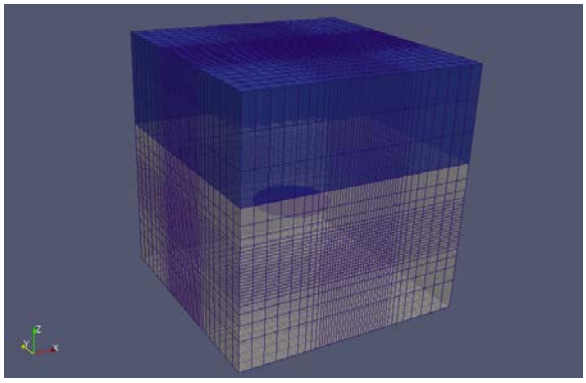

Figure 3: Grid with horizontal disc as a fracture cloud. The grid has 47,629 blocks.

3.3 Modelling procedure

Different clouds of fractures are considered in order to cover the range encountered in real stimulated reservoirs. Two main types of fracture clouds are presented: horizontal and vertical planar disks. In each case the first model considered has a fracture cloud in the form of a 2D disk. Then, for later models, the stimulated volume was increased, in the form of an approximate ellipsoid, until an almost spherical shape was achieved. Four geometries for each type of fracture were created. Figures 4 and 5 show the different clouds of fractures and Tables 2 and 3 summarise their characteristics. For most of the simulations discussed below the fracture cloud is treated as a single porosity, uniform porous medium, but numerical experiments were also conducted using a dual porosity representation.

Different arrangements of wells were simulated. According to Held *et al*. (2014), multi-well systems achieve a larger heat exchange surface than doublet systems. In this case the injection well is located at the centre of the stimulated area and the production wells are located close to the borders of the cloud. The five-spot well distribution is often used in the oil industry (Butler *et al*., 2004). Also, all the production wells are located above the injection area in order to let the cool water go down and the hot water move up, with the exception of the case where the fracture cloud is a horizontal disk.

In order to derive a qualitative understanding of the different horizontal clouds a second set of scenarios are modelled, where the injection well is located at the bottom of the fracture cloud, thus giving the maximum separation between the injection and productions points. In practice this would require the injection well to be deepened after reservoir stimulation.

Scenarios are also modelled for fractured disks of different sizes (radius of 400, 320 and 280 meters) and higher permeability (100 times original). Also the case of a constant injection pressure is considered.

For most scenarios all the lateral boundaries of the model are sealed and so all the fluid loss occurs ultimately through the surface. Scenarios with lateral recharge are also considered later in this work.

The production wells operate on deliverability with the mass flow proportional to the difference between the current feed-block pressure and the original block pressure. The coefficient of proportionality is a productivity index (PI) times the fluid mobility. Thus all the production wells start production as soon as the pressure in the block where they are located reaches a pressure higher than the hydrostatic pressure in the same block in the natural state model.

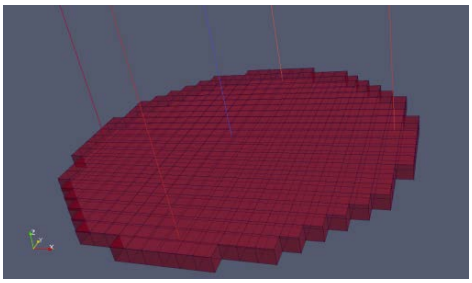

Disc

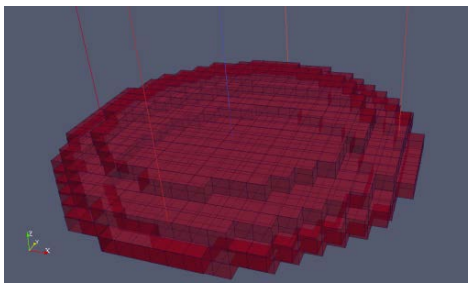

Ellipsoid 1

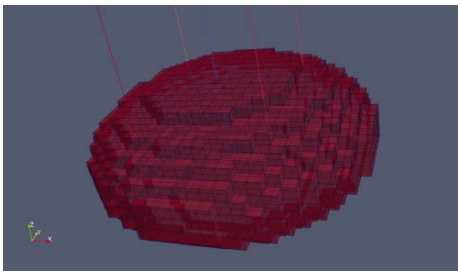

Ellipsoid 2

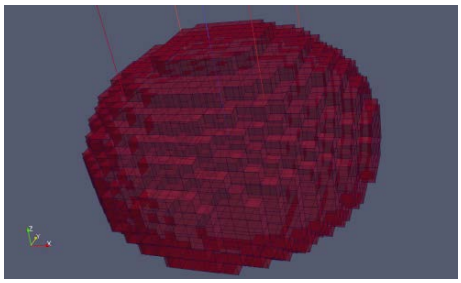

Ellipsoid 3

Figure 4: Clouds of fractures – horizontal axis.

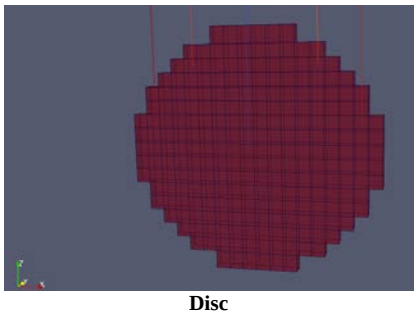

Disc

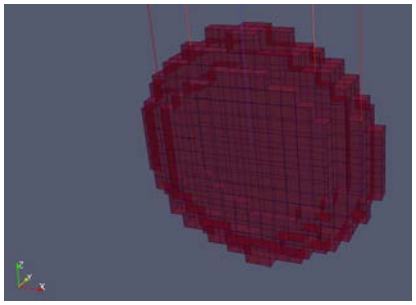

Ellipsoid 1

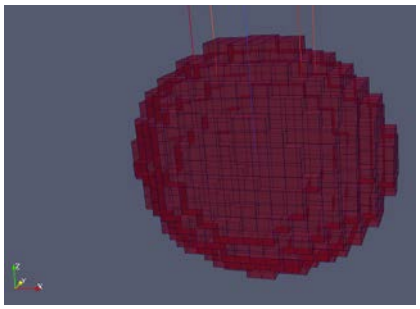

Ellipsoid 2

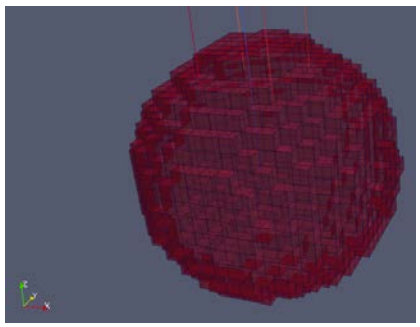

Ellipsoid 3

Figure 5: Clouds of fractures – vertical axis.

Table 2: Geometry of the cloud of fractures. Horizontal axis

Cloud	Volume (10^6 m^3)	Disc radius/Ellipsoid radius (m)
Disc	28.6	480 / -
Ellipsoid 1	110.3	480 / 117
Ellipsoid 2	224.5	480 / 234
Ellipsoid 3	338.3	480 / 350

Table 3: Geometry of the cloud of fractures. Vertical axis

Cloud	Volume (10^6 m^3)	Disc radius/Ellipsoid radius (m)
Disc	15.4	350 / -
Ellipsoid 1	59.0	350 / 117
Ellipsoid 2	120.3	350 / 234
Ellipsoid 3	181.1	350 / 350

Each scenario was modelled for a 25 years period and the parameters to be studied are calculated as follows:

- The water loss is calculated by:

$$\%\dot{m}_{inj} = \frac{\dot{m}_{inj} - \dot{m}_p}{\dot{m}_{inj}}$$

- The enthalpy gain is calculated by:

$$\%h_p = \frac{h_p - h_{inj}}{h_{inj}}$$

Here $\dot{m}_{inj}$ and $\dot{m}_p$ stands for injection and production mass flow rate, respectively. In the same way h_{inj} and h_p stands for injection and production enthalpies.

For simplicity, all the production values are averaged in time. The total heat output is the sum of the heat output of each well. In the same way, the total of production mass flow rate is the sum of the flow rate for each well. The average enthalpy is calculated as the division of the total power by the total mass flow.

The efficiency of the power plant is assumed to be an average of 8%, as some of that electricity is required to pump water into the enhanced reservoir. It is not within the scope of this paper to consider the selection of the best pump system, but an average pump system efficiency of 60% is considered.

3.4 Parameters to be varied

As explained above, one of the parameters to be varied is the numbers of production wells. A second important parameter is the injection rate. These are probably the key variables determining the performance of an EGS project. Every scenario is simulated with a constant injection rate in the range of 5 – 30 kg/s. The injected water is assumed to be a mixture of the rejected water from the binary plant and a new supply of make-up water, required because of the losses from the reservoir.

The temperature of the injected water depends on the temperatures of both fluids coming into the mixture. On one hand the temperature of the rejected water from the power plant depends mainly on the silica saturation index at the outlet from the heat exchanger. This should be less than 2 (Zarrouk, Woodhurst, & Morris, 2014) for a binary power plant. On the other hand the temperature of the make-up water will depend on the ambient temperature. For simplicity the injection water is fixed at approximately sixty degrees Celsius equivalent to an enthalpy of 251.2 kJ/kg.

3.5 Natural state model

The natural state model is achieved by running the simulation for more than thirty million years regardless of the initial conditions of the system. A background heat flux of 250 mW/m^2 is applied at the bottommost layer in the model. No other sources of heat or mass are introduced in the model. The natural state temperature gradient is shown in Figure 6. The two lines represent the temperature gradient in the sediments (blue) and granite (red) layer, with values of 11°C/km and 9°C/km, respectively. The temperature is uniform in the horizontal plane.

The pressure distribution, corresponding to the hydrostatic pressure at those temperatures, gives a pressure at the center of the fracture cloud of approximately 185 bars.

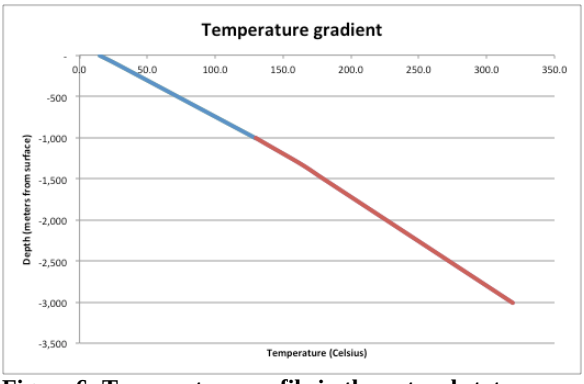

Figure 6: Temperature profile in the natural state.

4. RESULTS

4.1 Power production

Contour plots of power production as a function of injection rate and the number of production wells are shown in Figures 7 and 8. Only the results for the "disc" and "ellipsoid 3" fracture clouds are presented. Similar results were obtained for the other fracture clouds. The plots show that the increase in power production is not a linear function of injection rate and the number of production wells, as explained by analysing the water loss and enthalpy gain.

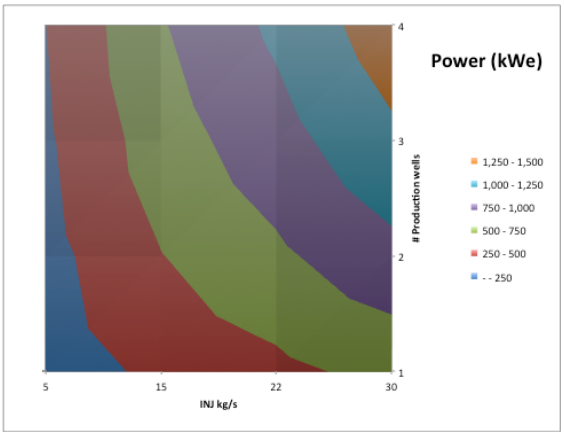

Disc

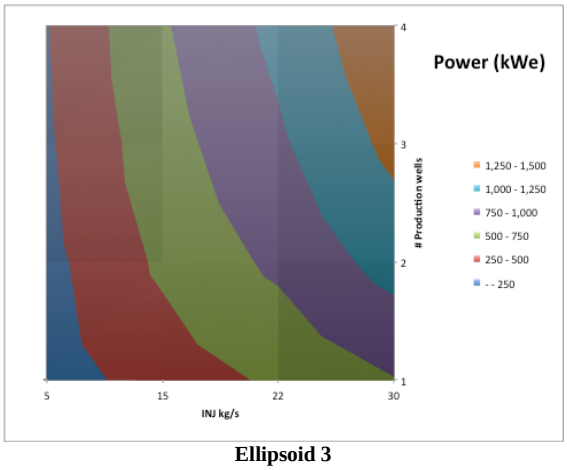

Ellipsoid 3

Figure 7: Power output for models with horizontal fracture clouds.

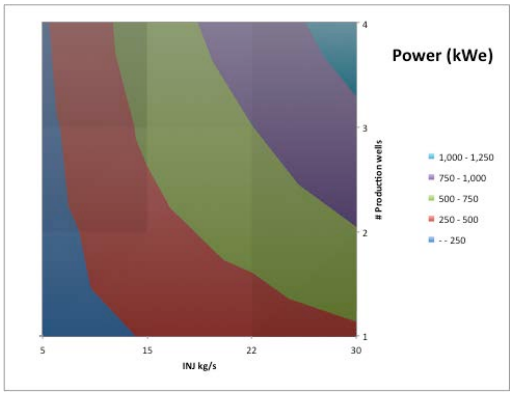

Disc

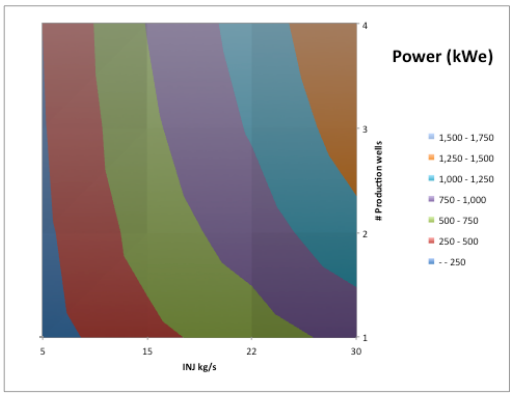

Ellipsoid 3

Figure 8: Power output for model with vertical fracture clouds.

The results show that the power production is directly dependent on the number of wells and the flow rate of the injected water. More wells and more water mean more heat mining, but the relationship is not linear, *i.e.* doubling the injection rate does not double the heat output.

A correlation can be obtained in order to provide a method for deciding if is it better to have more production wells or to increase the injection rate. The best-fit correlation has the following mathematical form:

$$P_e = \eta * \beta * \dot{m}_{inj}{}^{\propto_1} * x^{\propto_2}$$

Here "P_e" is the electrical power output in kW, "η" is the generation efficiency (estimated to be 8%), "$\beta, \propto_1, \propto_2$" are parameters to be estimated for each cloud, "$\dot{m}_{inj}$" is the mass injected and "x" is the number of injection wells. For the horizontal fracture clouds Table 4 shows the values obtained for those parameters and the range of electrical output obtained with the parameter values used in the simulations. Similar results were obtained for the vertical fracture clouds.

Table 4: Production parameters and range of electrical generation for horizontal fracture clouds.

Cloud	Parameters			Electrical power (MWe)	
	β	$\propto_1$	$\propto_2$	Min	Max
Disc	281	0.965	0.628	0.11	0.43
Ellipsoid1	313	1.003	0.543	0.13	1.61
Ellipsoid 2	328	1.008	0.490	0.13	1.6
Ellipsoid 3	300	1.014	0.496	0.12	1.5

The power output given in Table 4 does not consider pump requirements. Pump load depends on how much water has to be injected and the pressure of the reservoir that has to be overcome by the pump. In every scenario it is found that the pressure in the injection block increases rapidly until the maximum power output is achieved, and then the pressure increases slowly in comparison to the early behaviour. Table 5 shows the pump requirement for each geometry and injection rate.

Table 5: Pump power requirements for horizontal clouds in a doublet system (kWe).

Cloud	Injection rate (kg/s)			
	5	15	22	30
Disc	21	207	457	879
Ellipsoid 1	13	127	281	534
Ellipsoid 2	13	124	270	509
Ellipsoid 3	13	122	270	509

In order to understand the behaviour discussed above it is useful to analyse how much water is going to be produced and, thus, how much water is going to be needed from another source. Figure 9 shows water loss versus the number of production wells at various injection rates. The plots show that the water loss decreases as the number of production wells increases but the injection rate makes very little difference. The water loss is less for the larger Ellipsoid 3 fracture cloud than for the Disc

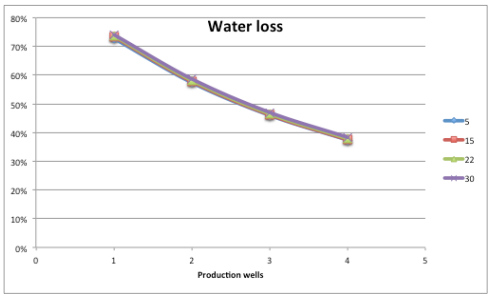

Disc

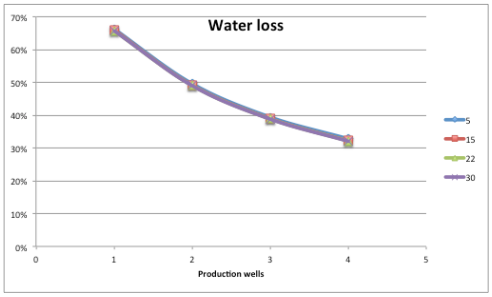

Ellipsoid 3

Figure 9: Water losses in horizontal fracture clouds

4.2 Production profiles

The analysis above applies to average values of the parameters, but it is also important to investigate the behaviour over time. For every scenario, it takes a short time to reach the maximum power output. The maximum injection pressure is reached at the end of the production time and no boiling is observed. It is observed that for a given geometry with a given number of production wells the "decline" stage arrives sooner with higher injection rates.

Figure 10 shows the thermal power output of a horizontal disc cloud, for two production wells and an injection rate of 15 kg/s. It can be seen that each production well has a different production profile, but what it is actually used at the power plant is the average output of both of them combined. The difference between the performances of the wells can be explained by their locations since the wells closer to the injection well receive cooler water sooner giving a lower production enthalpy. On the other hand, wells closer to the injection well show a slightly higher mass flow rate.

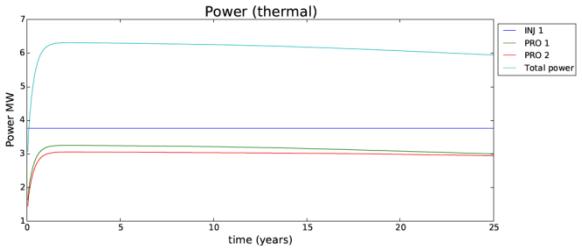

Figure 10: Power output. Horizontal disc, two production wells and injection rate of 15 kg/s.

The power decline is mainly due to a decrease in the enthalpy of the production fluid, and not due to water loss. Figures 11 and 12 show the profiles of mass production and flowing enthalpy for the case shown in Figure 10.

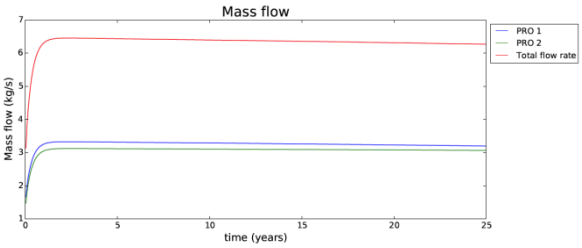

Figure 11: Mass flow. Horizontal disc, two production wells and injection rate of 15 kg/s

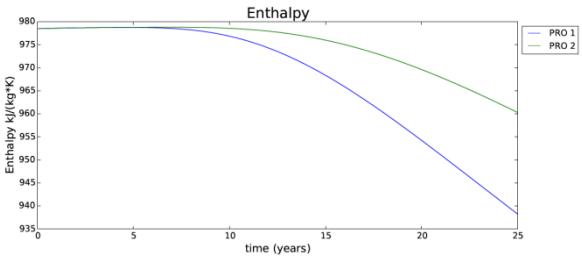

Figure 12: Flowing enthalpy. Horizontal disc, two production wells and injection rate of 15 kg/s

4.3 Enthalpy

The enthalpy gain depends on flow rate, the number of wells and their locations. For a given geometry, the injected fluid moves radially (Kohl & Mégel, 2007) until it goes through the most permeable structure. As the permeability is the same in every direction the fluid tends to go directly to the production wells. Thus, the heat is mined from the injection point to the production point. As soon as the cold front reaches the production point, heat production will rapidly decline. For the case of the "disc", with one production well, the production enthalpy remains stable with time, but if injection occurs at a higher flow rate, say at 30 kg/s, starting from the fifth year, enthalpy decreases rapidly (Figure 13).

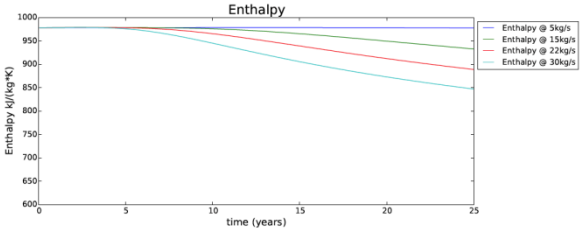

Figure 13: Flowing enthalpy in a horizontal disc, one production well.

For some fracture clouds, with the productions wells above the injection well, the effect of the temperature gradient on the produced fluid is noticeable. The injected fluid pushes the hot fluid from the injection well towards the production, giving flowing enthalpies at the production wells higher than the original value at that depth. The flowing enthalpies of the horizontal clouds are showed in Figure 14

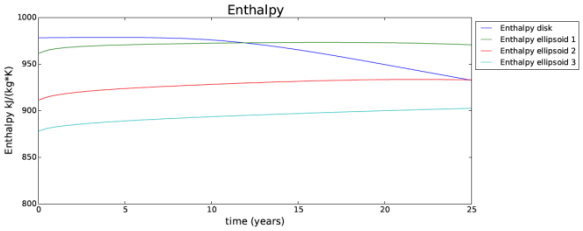

Figure 14: Flowing enthalpy in horizontal clouds with one production well and injection rate of 15 kg/s

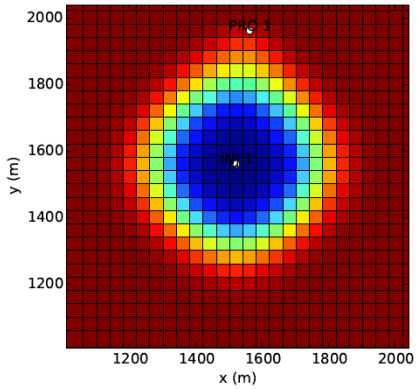

One production well

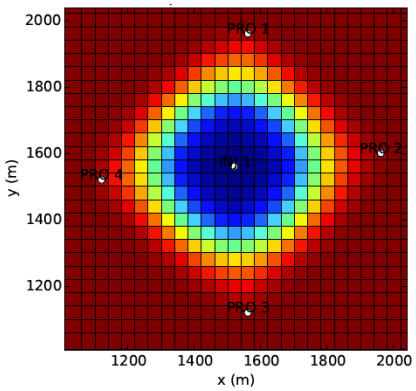

Four production wells

Figure 15: Temperature distribution in a horizontal disc with an injection rate of 15 kg/s

4.4 Temperature distribution

Figure 15 shows the temperature distribution at the end of the production period (year 25) for the horizontal disk with either one or four production wells. It can be seen that the

injected fluid mines the heat radially, starting from the injection point.

In Figure 16, it can be seen that the injected fluid does not expand very far vertically into the non-stimulated area.

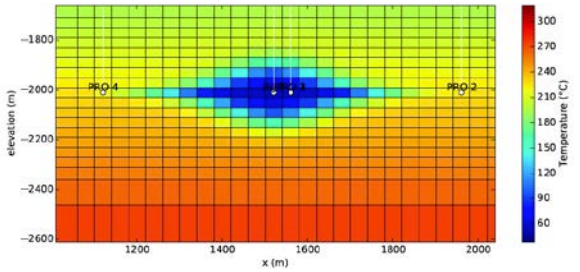

Figure 16: Vertical slice through the horizontal disc, four production wells and an injection rate of 15 kg/s

4.5 Better permeability enhancement

The base case used a ten-fold enhancement of the original permeability. Additionally, a scenario of a hundred-fold enhancement was modelled and some of the results are shown in Figure 17. It shows that with a more permeable fracture cloud, to generate the same power, less injection water is needed.

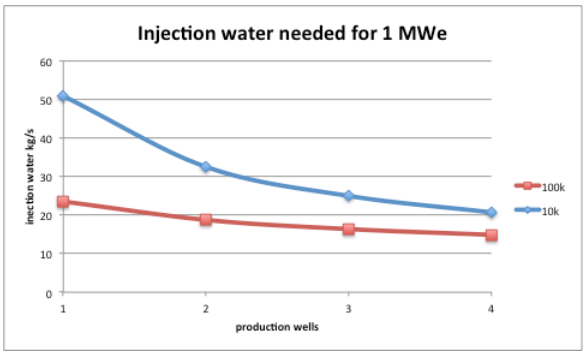

Figure 17: Injection water needed for 1 MWe, ten- and hundred-fold permeability enhancement. Horizontal disc.

5. CONCLUSIONS

In order to know what to expect in terms of power generation from an EGS project with different shapes of clouds of fractures several correlations were made for range of injection rates of 5 – 30 kg/s and 1 to 4 production wells with one injector in the centre. The power output range goes from 100 kWe to 1.6 MWe, not including the pumping power. In some cases, such as for the horizontal disc, more pumping power is required than is generated by the power plant. Even a project producing 1.6 MWe with a required pumping power of 0.5 MWe is unlikely to be economically feasible for a 5 well system.

Also correlations for water losses have been developed. The percentage of injected water lost mainly depends on the number of production wells and the shape of the cloud of fractures. It is found that if the permeability of the cloud is higher then there are smaller water losses, but this effect is diminished when more production wells are used. Thus, the drilling of more production wells could avoid the necessity of re-stimulating a geothermal system. Likewise, in smaller clouds less water losses are found.

In terms of maintaining the production enthalpy the best configuration found was the horizontal ellipsoid 3, where the production wells are 4 layers (160 meters) above the injection well. The higher elevation production wells gives a more stable production temperature (also lower) than if the production wells are at the same depth as the injection well. In the models where the injection well was deepened no significant changes in production enthalpy were found. This means that it is better to drill as deep as possible in the first place, and drilling again in the future might be pointless.

REFERENCES

Bataillé, A., Genthon, P., Rabinowicz, M., & Fritz, B.: Modeling the coupling between free and forced convection in a vertical permeable slot: Implications for the heat production of an Enhanced Geothermal System. *Geothermics*, *35*(5-6), 654–682. (2006).doi:10.1016/j.geothermics.2006.11.008

Brown, D.W.: Hot dry rock geothermal energy: important lessons from Fenton Hill. *Proceedings*, Thirty-Fourth Workshop on Geothermal Reservoir Engineering, Stanford University, Stanford, California, Feb. 9–11, (2009).

Butler, S. J., Sanyal, S. K., & Robertson-Tait, A.: A Numerical simulation study of the performance of enhanced geothermal systems. *Proceedings*, Twenty-Ninth Workshop on Geothermal Reservoir EngineeringStanford University, Stanford, California, Jan. 26-28, (2004).

Chamorro, C. R., García-Cuesta, J. L., Mondéjar, M. E., & Pérez-Madrazo, A.: Enhanced geothermal systems in Europe: An estimation and comparison of the technical and sustainable potentials. *Energy*, *65*, 250–263. (2014).doi:10.1016/j.energy.2013.11.078

Chen, D. and Wyborn, D.: Habanero field tests in the Cooper Basin, Australia: A proof-of-concept for EGS. GRC *Transactions*, 33, 159-164. (2009).

Genter, A., Fritsch, D., Cuenot, N., Baumgartner, J. and Graff, J-J.: Overview of the current activities of the European EGS Soultz project: from exploration to electricity production. *Proceedings*, Thirty-Fourth Workshop on Geothermal Reservoir Engineering, Stanford University, Stanford, California, Feb. 9-11, (2009).

Gentier, S., Rachez, X., Peter-Borie, M., Blaisonneau, A. and Sanjuan, B.: Transport and flow modelling of the deep geothermal exchanger between wells at Soultz-sous-Forets (France). GRC *Transactions*, 35, 363-369. (2011).

Held, S., Genter, A., Kohl, T., Kölbel, T., Sausse, J., & Schoenball, M.: Economic evaluation of geothermal reservoir performance through modeling the complexity of the operating EGS in Soultz-sous-Forêts. *Geothermics*, *51*, 270–280. (2014).

Hogarth, R.A. and Bour, D.: Flow performance of the Habanero EGS closed loop. *Proceedings*, World Geothermal Congress 2015, Melbourne, Australia, 19-25 April, (2015).

Holl, H-G. and Barton, C.: Habanero field - structure and state of stress. *Proceedings*, World Geothermal Congress 2015, Melbourne, Australia, 19-25 April, (2015)..

Jiang, F., Luo, L., & Chen, J.: A novel three-dimensional transient model for subsurface heat exchange in enhanced geothermal systems. *International Communications in Heat and Mass Transfer*, *41*, 57–62. (2013).

Kohl, T., & Mégel, T.: Predictive modeling of reservoir response to hydraulic stimulations at the European EGS site Soultz-sous-Forêts. *International Journal of Rock Mechanics and Mining Sciences*, *44*(8), 1118–1131. (2007). doi:10.1016/j.ijrmms.2007.07.022

Llanos, E. M., Zarrouk, S. J., & Hogarth, R. A.: Numerical model of the Habanero geothermal reservoir, Australia. *Geothermics*, *53*, 308–319. (2015).

McMahon, A., & Baisch, S.: Case of study of the seismicity associated with the stimulation of the enhanced geothermal system at Habanero, Australia. *Proceedings*, Australian Geothermal Energy Conferences 2013, Brisbane, Australia, 14-15 November, (2013).

Mills, T., & Humphreys, B.: Habanero Pilot Project - Australia ' s First EGS Power Plant. *Proceedings*, Australian Geothermal Energy Conferences 2013, Brisbane, Australia, 14-15 November, (2013).

Pritchett, J. W.: Estimating "Technical Capacity" for Geothermal Electricity Generation in the United States. GRC *Transactions*, 36, 535-538. (2012).

Pruess, K.: Enhanced geothermal systems (EGS) using CO2 as working fluid-A novel approach for generating renewable energy with simultaneous sequestration of carbon. *Geothermics*, *35*(4), 351–367. (2006).

Pruess, K., Oldenburg, C., & Moridis, G.: TOUGH2 User's Guide, Version 2.0. *Lawrence Berkeley National Laboratory Report*, *LBNL-43134*. (1999).

Sausse, J., Dezayes, C., Dorbath, L., Genter, A., & Place, J.: 3D model of fracture zones at Soultz-sous-Forêts based on geological data, image logs, induced microseismicity and vertical seismic profiles. *Comptes Rendus - Geoscience*, *342*(7-8), 531–545. (2010). doi:10.1016/j.crte.2010.01.011

Siffert, D., Haffen, S., Garcia, M.H. and Geraud, Y.: Phenomenological study of temperature gradient anomalies in the Buntsandstein formation, above the Soultz geothermal reservoir, using TOUGH2 simulations. *Proceedings*, Thirty-Eighth Workshop on Geothermal Reservoir Engineering, Stanford University, Stanford, California, February 11-13, (2013).

Tester, J., Anderson, B., Batchelor, A., Blackwell, D., DiPippo, R., Drake, E., *et al.*: *The future of geothermal energy: impact of enhanced geothermal systems (EGS) on the United States in the 21st century. MIT*. (2006).

Wu, N.-Y., Zeng, Y.-C., & Su, Z.: Numerical simulation of heat production potential from hot dry rock by water circulating through two horizontal wells at Desert Peak geothermal field. *Energy*, *56*, 92–107. (2013). doi:10.1016/j.energy.2013.04.055

Yanagisawa, N., Rose, P. and Wyborn, D.: First tracer test at Cooper-Basin, Australia HDR reservoir. GRC *Transactions*, 33, 281-284. (2009).

Zarrouk, S. J., & Moon, H.: Efficiency of geothermal power plants: A worldwide review. *Geothermics*, *51*, 142–153. (2014). doi:10.1016/j.geothermics.2013.11.001

Zarrouk, S. J., Woodhurst, B. C., & Morris, C.: Silica scaling in geothermal heat exchangers and its impact on pressure drop and performance: Wairakei binary plant , New Zealand. *Geothermics*, *51*, 445–459. (2014). doi:10.1016/j.geothermics.2014.03.005

Zeng, Y. C., Wu, N. Y., Su, Z., & Hu, J.: Numerical simulation of electricity generation potential from fractured granite reservoir through a single horizontal well at Yangbajing geothermal field. *Energy*, *65*, 472–487. (2014). doi:10.1016/j.energy.2013.10.084

Zeng, Y. C., Wu, N. Y., Su, Z., Wang, X. X., & Hu, J.: Numerical simulation of heat production potential from hot dry rock by water circulating through a novel single vertical fracture at Desert Peak geothermal field. *Energy*, *63*, 268–282.